

Spin-polarized tunable photocurrents

Matías Berdakin,^{1,2,*} Esteban A. Rodríguez-Mena,^{3,*} and L. E. F. Foa Torres³

¹INFIQC (CONICET-UNC), Ciudad Universitaria, Pabellón Argentina, 5000 Córdoba, Argentina.

²Departamento de Química Teórica y Computacional, Fac. de Ciencias Químicas,

Universidad Nacional de Córdoba, Ciudad Universitaria, Pabellón Argentina, X5000HUA Córdoba, Argentina.

³Departamento de Física, Facultad de Ciencias Físicas y Matemáticas, Universidad de Chile, Santiago, Chile

(Dated: February 2, 2021)

Harnessing the unique features of topological materials for the development of a new generation of topological based devices is a challenge of paramount importance. Using Floquet scattering theory combined with atomistic models we study the interplay between laser illumination, spin and topology in a two-dimensional material with spin-orbit coupling. Starting from a topological phase, we show how laser illumination can selectively disrupt the topological edge states depending on their spin. This is manifested by the generation of pure spin photocurrents and spin-polarized charge photocurrents under linearly and circularly polarized laser-illumination, respectively. Our results open a path for the generation and control of spin-polarized photocurrents.

Introduction.— The early theoretical proposals [1–4] and the subsequent experimental realization of topological insulators [5, 6] have lined up the relentless scientific efforts of an ever growing community in Physics, Materials Science and Chemistry [7, 8]. Besides interesting features such as spin-momentum locking [9], topologically protected states are attractive because, unlike the usual electronic states in solids, they enjoy an intrinsic robustness to perturbations and disorder. But this lack of fragility opens up new challenges for their manipulation. Typical schemes such as surface functionalization [8] are quite ineffective when applied to topological insulators. The difficulty to cleanly turn-off conduction of charge and spin has motivated proposals for a topological field effect transistor [10–13] where the electric field drives a topological transition to a trivial insulating phase, a concept that has been experimentally realized recently [14].

Another stream of research has been looking to exploit light-matter interaction in materials to control their electrical properties. This includes generating effects such as dichroism [15, 16], a situation where electrons at different valleys absorb left and right-handed photons differently, which is of much relevance in the context of two-dimensional materials [17–19]. A different approach is aimed at using intense laser illumination to actually change the properties of the material [20]. Indeed, strong illumination has been demonstrated to produce hybrid electron-photon states [21, 22] (Floquet-Bloch states) which may present new topological properties [23–25] (see also Ref. [26]) and even exhibit a light-induced Hall effect [27].

Here, we study laser-illumination on graphene with spin-orbit coupling and a sublattice-symmetry breaking potential. The parameters are fixed so that, in absence of radiation, the system is in a topologically insulating phase with counter-propagating spin-polarized states protected by time-reversal symmetry. Previous related studies have focused on the rich phase diagram of Floquet topological phases under strong high-frequency radiation ($\hbar\Omega$ larger than the bandwidth) [28] and also considering resonant processes [29]. In contrast to those studies, here we focus on using light to gently disrupt the native topological states. In this regime one might ex-

pect an interesting interplay between symmetry breaking (inversion symmetry, or time-reversal symmetry which can be broken or preserved by circular or linearly polarized light), spin-orbit coupling which also intertwined the valley and spin degrees of freedom, and photon-induced processes. Specifically, we show that laser-illumination leads to: (i) pure spin currents under linearly polarized light, and (ii) spin polarized charge currents under circular polarization. In both cases the spin (i) and charge (ii) currents flow even at zero-bias voltage. We rationalize these pumping currents in terms of a selective hybridization of electron-photon states which is enriched by valley and spin-selective selection rules under circular polarization.

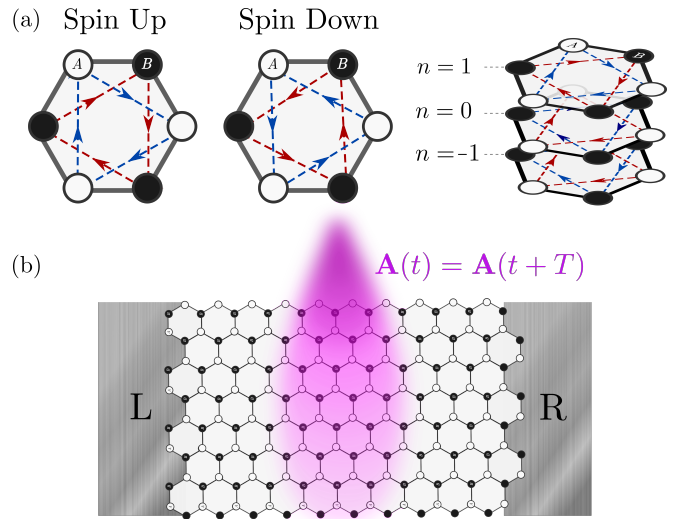


Figure 1. The irradiated Kane-Mele model. The system consists of two decoupled copies, each one representing spin up and spin down, and therefore they are time-reversal partners (a, left). Under the light spot, the system develops the replica scheme unfolding itself into several copies which represent photon dressed processes (a, right). In (b) a schematic representation of the device we will consider in the transport setup. Under particular conditions the transport of one spin might be suppressed while the remaining is *perfectly* unaffected.

In the following we present the lattice model we use to test our ideas, the basics of Floquet theory and the generalized Landauer-Büttiker formalism. Later on we present our results for the spectral and transport properties, rationalizing them in terms of a few main ingredients. Finally, we discuss possible realizations and potential application of these ideas as well as drawbacks that may arise on the realization of these concepts.

Hamiltonian model for Floquet-Kane-Mele system.— Let us now consider the Hamiltonian for graphene with a staggering potential and intrinsic spin-orbit (ISO) interaction [1]:

$$\begin{aligned} \mathcal{H}_0 = & \sum_{i,s_z} E_i c_{i,s_z}^\dagger c_{i,s_z} - \gamma_0 \sum_{\langle i,j \rangle, s_z} c_{i,s_z}^\dagger c_{j,s_z} - \\ & - i\gamma_{SO} \sum_{\langle\langle i,j \rangle\rangle, s_z} \nu_{i,j} s_z c_{i,s_z}^\dagger c_{j,s_z}, \end{aligned} \quad (1)$$

where c_{i,s_z}^\dagger and c_{i,s_z} are the creation and annihilation operators for electrons on the π -orbital on site i with spin up $s_z = 1$ or spin down $s_z = -1$. γ_0 is the nearest-neighbors matrix element and γ_{SO} is the intrinsic spin-orbit coupling. We set $\gamma_0 = 1$ as our energy scale. $\nu_{i,j}$ is +1 (−1) if the path from j to i is clockwise (anticlockwise), as shown in Fig. 1a (right for spin up, left for down). The on-site energies E_i are chosen equal to Δ (− Δ) for the sites on the A (B) sublattice. The single and double brackets denote that the summation is over first or next nearest-neighbors. Although the spin-orbit coupling in bare graphene is too small, the same physics can be realized in other two-dimensional materials such as silicene and germanene [30] where this coupling is stronger.

The effect of laser illumination is captured through the Peierls' substitution [31, 32], a time dependent phase in the nearest-neighbors and next-nearest-neighbors matrix elements:

$$\gamma_{i,j}(t) = \gamma_{i,j}^{(0)} \exp \left[i \frac{2\pi}{\Phi_0} \int_{\mathbf{r}_j}^{\mathbf{r}_i} \mathbf{A}(t) \cdot d\mathbf{r} \right]. \quad (2)$$

where $\gamma_{i,j}^{(0)}$ are the unperturbed matrix elements as given in Eq. 1, Φ_0 is the magnetic flux quantum and $\mathbf{A}(t)$ is the vector potential. For a monochromatic plane wave in the z -direction (perpendicular to the graphene sheet) we consider $\mathbf{A}(t) = A_0 \cos(\Omega t) \hat{x} + A_0 \sin(\Omega t + \phi) \hat{y}$, where Ω is the radiation frequency, A_0 determines the driving amplitude and $\phi = 0, \pm\pi/2$ controls the polarization linear or left/right hand polarized, respectively. Right hand polarization is considered whenever we mention circular polarization. The laser strength can be characterized by the dimensionless parameter $z = A_0 a 2\pi / \Phi_0$.

Similar systems were considered before with a few differences: Ref. [33] studied laser-illuminated transition metal dichalcogenide without spin-orbit coupling considered here, and Refs. [29, 34] studied germanene and silicene in the high-frequency regime while here we focus on frequencies smaller than the bandwidth. Other studies using Floquet theory focused on the topological states induced by light [35–37],

rather than the modification of native topological states considered here.

Floquet theory for the spectral and transport properties.—

Floquet theory allows for a non-perturbative and non-adiabatic solution of problems involving a time-periodic Hamiltonian such as ours satisfying $\mathcal{H}(t) = \mathcal{H}(t + T)$ with $T = 2\pi/\Omega$. The Floquet theorem assures that there is a complete set of solutions of the form $|\psi_\alpha(t)\rangle = \exp(-i\varepsilon_\alpha t) |\phi_\alpha(t)\rangle$, where ε_α are the quasienergies and $|\phi_\alpha(t + T)\rangle = |\phi_\alpha(t)\rangle$ are the Floquet states obeying:

$$\mathcal{H}_F |\phi_\alpha(t)\rangle = \varepsilon_\alpha |\phi_\alpha(t)\rangle, \quad (3)$$

where $\mathcal{H}_F \equiv \mathcal{H} - i\partial/\partial t$ is the Floquet Hamiltonian. Thus, one gets an eigenvalue problem in the direct product space (Floquet or Sambe space [38]) $\mathcal{R} \otimes \mathcal{T}$ where \mathcal{R} is the usual Hilbert space and \mathcal{T} the space of T -periodic functions spanned by $\langle t | n \rangle = \exp(in\Omega t)$. The index n is often called the *replica* index and can be associated to different photon channels. In this picture, an electron entering lead α in a given reference replica n_0 can scatter to lead β in replica m , thus exchanging $n = m - n_0$ quanta of the time-dependent modulation. Since asymptotically the different replicas are decoupled (as the time-modulation is limited to the sample), the total transmission probability from α to β , $\mathcal{T}_{\beta,\alpha}(\varepsilon)$, can be obtained by summing the probabilities associated to each of these processes (denoted with $\mathcal{T}_{\beta,\alpha}^{(n)}(\varepsilon)$):

$$\mathcal{T}_{\beta,\alpha}(\varepsilon) = \sum_n \mathcal{T}_{\beta,\alpha}^{(n)}(\varepsilon), \quad (4)$$

These probabilities can be computed using standard Green's functions techniques [32, 39, 40]. In a two-terminal setup in the lineal response regime (small bias voltage), the time-averaged current is given by [41]:

$$\bar{I} \simeq \frac{2e^2}{h} \mathcal{T}_+(\varepsilon_F) V + \frac{4e}{h} \int \mathcal{T}_-(\varepsilon) f(\varepsilon) d\varepsilon. \quad (5)$$

where $\mathcal{T}_\pm = (\mathcal{T}_{R,L} \pm \mathcal{T}_{L,R})/2$, $f = f_L + f_R$ is the sum of the Fermi distribution functions at each lead (L or R) and V is the bias voltage. The second term on the right-hand side corresponds to a *pumping current* arising because of the asymmetry of the transmission coefficients. This current remains even at zero bias voltage (and it may even flow against an applied voltage). Such currents have been studied extensively in the past [42–45] and more recently have applied to the context of the shift photocurrents problem [46]. As we will see later on, in our case these pumping currents can be tuned by the interplay between the native topological states of the system, the laser polarization and photon assisted processes.

Quasi-energy dispersion. Let us start our discussion by analyzing the dispersion relations for a ribbon of laser-illuminated graphene with spin-orbit coupling and a staggering potential. This is shown in Fig. 2 for linear (c-d) and circular (e-f) polarization and also without radiation (a-b). Without

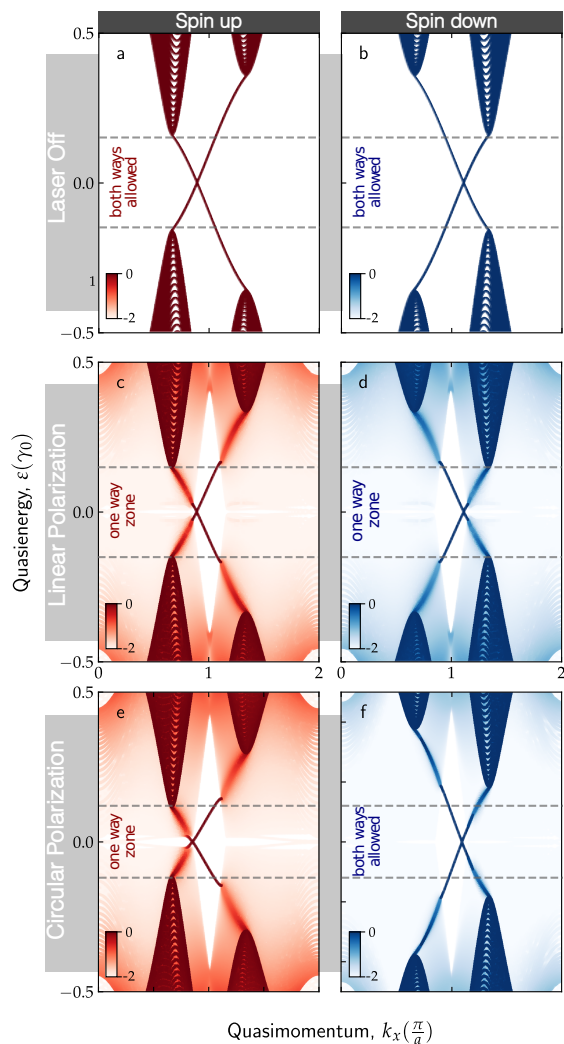


Figure 2. Spin resolved bandstructure of a honeycomb ribbon with intrinsic spin-orbit coupling. Computation performed over a zigzag nanoribbon of width $W = 100a$ (~ 25 nm). Panels (a-b) without irradiation. Panels (c-d) and (e-f) for linear and circular polarized irradiation, respectively. Red(blue) denote spin up(down). We consider $\Delta = 0.1$, $\gamma_{SO} = 0.05$, $\hbar\Omega = 1.5$ and $z_x = z_y = 0.15$. One or both ways allowed transport is highlighted for edge states bridge the energy gap. The color scale in the bottom shows the time-averaged density of states in log-scale.

radiation, when the spin-orbit term dominates over the staggering one has the expected topological states bridging the gap. The staggering is responsible for the asymmetry between the valleys, while the overall time-reversal symmetry enforces the mirror symmetry between the plots (when exchanging k by $-k$) for the different spin-components. The color scale encodes the contribution of each state to the time-averaged density of states [23] which is given by the weight of each state on the reference replica ($n = 0$), which is uniform and equal to unity in absence of radiation. For linear and circular polarization, the lighter tones (notice the log scale) show the regions with states due to the other replicas (each shifted by $\hbar\Omega$). Ra-

diation will introduce a coupling between the replicas (or, in other words, a coupling between a state with a given k at energy ε and other states at the same k with energy $\varepsilon + n\hbar\Omega$). The effect of such coupling is the hybridization of the native topological states of this system with the continuum provided by the replicas. In the figure this is evidenced as regions where the lines bridging the gap become blurred (the log scale emphasizes these regions which in normal scale will be hardly visible). Later on, we will see how transport is disrupted due to this hybridization.

Notice that the hybridization with the continuum appearing here is different from that studied in Refs. [47–49] where the continuum is provided by the states of a second layer in bilayer graphene. In contrast, here this is due to coupling with the continuum in other replicas through photon-assisted processes. Furthermore, spin plays a crucial role in the selection rules as we will highlight later on.

When comparing the results for linear and circular polarization in Fig. 2 we find an interesting asymmetry: while with linearly polarized light time reversal symmetry is preserved, circular polarization breaks it. The panels for spin up and down in Fig. 2e-f do not mirror each other as when TRS is preserved (panels c-d) and the response is thus expected to be spin-selective. As we will see next, this leads to a deeper selection rule tied to a spin-dependent circular-dichroism effect.

Transport properties.— Let us now turn to the transport properties. We consider a two-terminal setup where a central region is being illuminated while the leads remain in equilibrium. All the Hamiltonian parameters of the scattering zone and leads are equal. By using Floquet scattering theory as mentioned earlier, we compute the total transmission probabilities as a function of the energy of the incident electrons (ε). Furthermore, we can resolve the contributions of both spin components as shown in Fig. 3a-d (readers can find a detailed comparison between Floquet bandstructure and transport signatures in the supporting information). While without laser illumination one would expect a perfect and reciprocal transmission equal to unity for energies within the bulk gap, here we see a different picture. First, the left-to-right and right-to-left transmission probabilities differ, as is usual in driven systems with broken symmetries. But interestingly, the response is also highly sensitive to the spin component for circularly polarized light: the results show that one spin component gets stronger scattering (deviations from unity) while the other is less affected. This startling difference in the response for different spins (this is, the difference between Figs. 3c-d) begs for an explanation.

The results for the current, which we can resolve in its spin components are shown in Fig. 3 e (linear polarization and f (circular polarization). A first fact advanced earlier is that because of the non-reciprocity, there is a photo-generated current that appears even at zero bias voltage. This type of pumped current [42] or photocurrent in this case [46] is intertwined with the symmetry breaking induced by the different terms in the Hamiltonian. While inversion symmetry is broken in all cases (due to the staggering term), for linear polarization TRS

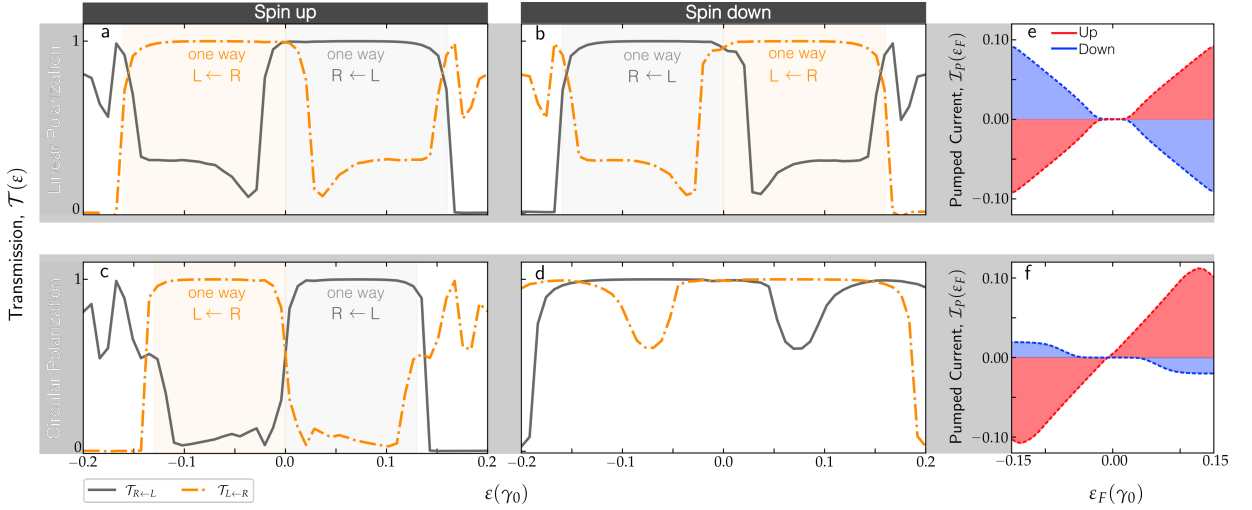


Figure 3. Effective transport properties for the scattering process averaged over one irradiation period. Parameters are the same than in Figure 2. Panels (a-d) show the transmission probabilities within the native gap. One-way charge transport is achieved in (a), (b) and (c) while in (d) no one-way effect is witnessed. Remarkably, the difference between both polarizations can be understood in terms of the circular dichroism on each copy of Haldane model. Panels (e-f) present the spin-resolved pump currents obtained for linear and circular polarization. Due to the presence of pumping currents in Floquet context, this behavior translates into a zero charge pumping with linear polarization yielding pure spin currents (e) while with circular polarizations (f) one can achieve spin polarized charge currents. The former can be tweaked by changing from right-hand to left-hand circular polarization.

is preserved and hence no net charge current can flow in this spinful case. The current per spin component is non-vanishing as shown in Fig. 3e, and together both components give a pure spin current.

In contrast, for circular polarization there is a non-vanishing current which turns out to be spin-polarized (see Fig. 3f). The polarization depends on the Fermi energy, being almost perfect close to the charge neutrality point and of about 83% at higher/lower energies. The spin-selective non-reciprocity (Figs. 3c-d) under circular polarization together with the spin-polarized photocurrents (Fig. 3f) are the main numerical results of this paper. Notice that the spin polarization can be inverted by changing the handedness of the laser polarization.

To rationalize the transport results and the quasienergy dispersions we now discuss several points that altogether explain our findings. But first, we need to dig deeper by presenting the different contributions to the total transmissions shown in Fig. 3. Indeed, an electron entering the illuminated sample with energy ϵ can exit elastically (without emitting or absorbing a net number of photons) or inelastically. The partial transmissions $\mathcal{T}_{i,j}^{(n)}$ for linear and circular polarization are shown in Fig. 4 and a discussion of the role of the inelastic back scattering can be found in the supplementary information. The insets of Fig. 4 show the transition matrix elements between the unperturbed initial and final states. These insets confirm our previous observation that the propagating state with spin down traversing the device is much less disturbed by circularly polarized light than the other.

The following general points explain the observed numerical features:

1. *Generalized symmetry in Floquet space.* The following

relation among transmission probabilities is verified in our case:

$$\mathcal{T}_{\beta,\alpha}^{(n)}(\epsilon) = \mathcal{T}_{\alpha,\beta}^{(-n)}(-\epsilon). \quad (6)$$

This is enforced by an underlying symmetry in Floquet-space:

$$\Gamma \mathcal{H}(\mathbf{k}) \Gamma^\dagger = -\mathcal{H}(\mathbf{k})^*, \quad (7)$$

where $\Gamma = \sigma_y K$, K being the complex conjugation operator. This generalized symmetry thus inverts the energy sign while mirroring the space and replica coordinates. This symmetry, which is fulfilled in our device setup, therefore links the transmission probabilities in the different panels of Figs. 3 and 4, which also serves as a numerical test of our results. We note that the similar relations have also been used in a different context in Floquet systems [50].

2. *Spin-selective dichroism effect: a selection rule linking Chern number, circular polarization handedness and spin.* Under illumination with circularly polarized light we observe a marked transport asymmetry between spin components, and also within the same spin subspace when the handedness of the laser polarization changes. The latter is commonly referred to as circular dichroism. The existence of circular dichroism in the presence of both a complex next-nearest-neighbor coupling and a staggering potential for the bulk states has been discussed in Ref. [51]. In that reference, Ghalamkari and coauthors find that there is a selection rule which ties the Chern number of the topological phases found

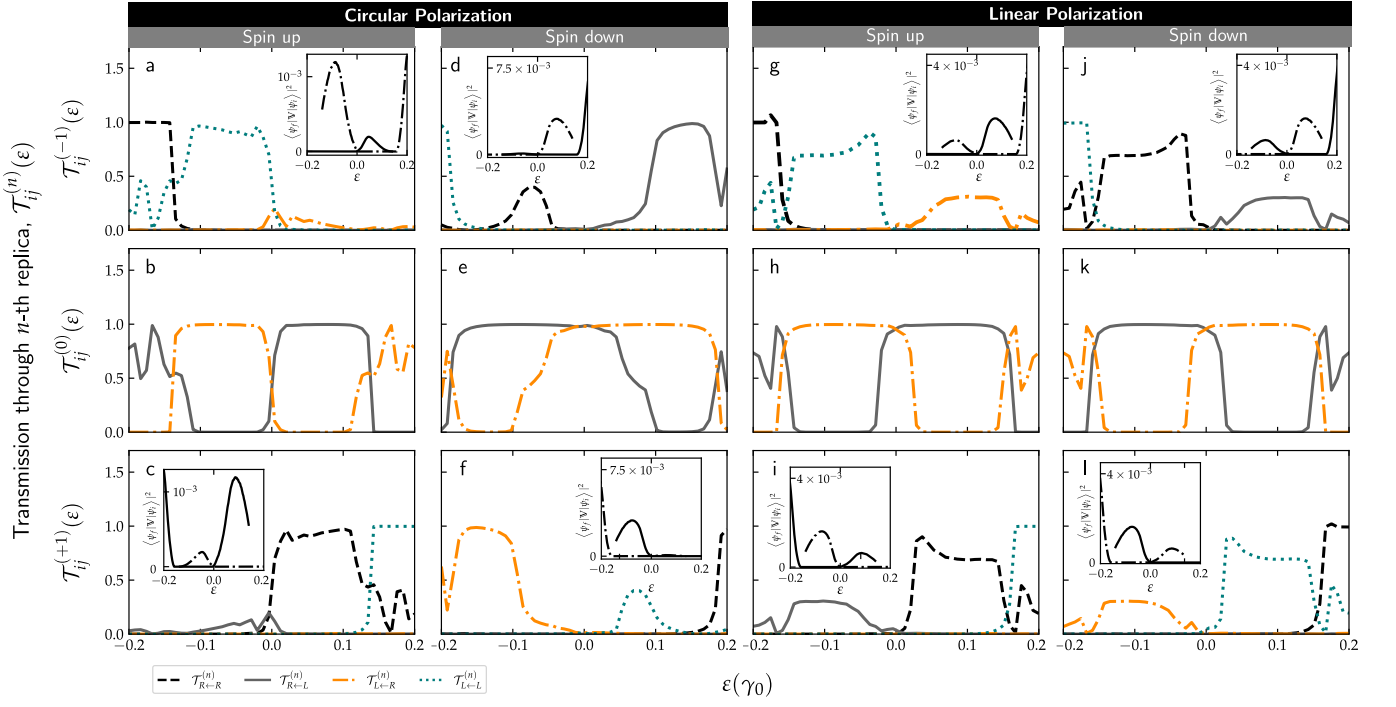


Figure 4. Detailed transmission probabilities averaged in time. Here, $\mathcal{T}_{ij}^{(n)}(\epsilon)$ stands for the transmission through a channel mediated by an exchange of n photons with an electron incident with quasienergy ϵ . From panels (a) to (f) circular polarization transport is shown, describing the whole process for each spin channel independently. From panel (g) to (l) the same information is depicted for linear polarization. Elastic channels prove to be the main source of transmission, while reflection processes, leading to a one-way transport in regions within the bulk gap, are completely mediated by photon-dressed processes, a distinctive signature of hybridization of the states with the continuum. Insets on each panel quantify the degree of coupling of a native topological state and the bulk bands states induced by higher order replicas. In the insets, solid and dashed lines represent opposite edge chiral states.

in the Haldane model [52] with a distinctive response to left and right circular polarization.

In our case, when looking at each spin component separately, our numerical results show that this selection rule persists for a finite system, when the transitions include an edge state and a state in the bulk spectrum. Furthermore, the fact that both spin components are related by time-reversal in \mathcal{H}_0 produces an inversion of the circular dichroism when passing from spin up to spin down, since it follows the sign inversion of the spin-resolved Chern number. Here we observe that this inversion of the circular dichroism is also fulfilled for the finite system, a fact which one might intuitively tie in with the bulk-boundary correspondence.

3. *Hybridization of edge states with the continuum provided by a different Floquet replica.* The selection rule stated in point 2 plays a crucial role in establishing the possible light-induced transitions among the electronic states. For Fermi energies within the bulk gap of the sample, thanks to photon-assisted processes, the topological edge states at ϵ can now transition towards the continuum of states at $\epsilon + n\hbar\Omega$ (where the system is un-gapped). Based on point 2, this hybridization with the states of a different replica is expected to be insensitive

to the spin for linear polarization but not for circular polarization. This is verified by numerically computing the modulus squared of the matrix element of the perturbation among the initial and final states, see insets of Fig. 4.

For our numerical simulations we employed a general model with staggering potential and spin-orbit coupling compatible with Germanene and Stanene, but we notice that the interplay between the staggering strength, the spin-orbit coupling and the laser frequency allows for a broad range of materials where the predicted photocurrents could be observed. Indeed, we require a system with with broken inversion symmetry hosting topological states. Within the Kane-Mele model this means that $2\Delta/\gamma_{SO} < 3\sqrt{3}$ [1, 52]. Furthermore, for the hybridization of the topological states with the continuum of the Floquet replicas to occur, the photon energy needs to be not smaller than the bulk gap of the non-irradiated system and not so large so that there are no continuum states $\hbar\Omega$ above a given energy. Fortunately, these conditions do not impose a restriction within the experimentally relevant regime of laser frequencies spanning from the mid-infrared to the visible range (see supplementary information). On the other hand, the temperature needed for the experimental realization and the fine-tuning of the irradiation condition will depend on the energy gap of the unperturbed material. The required laser

intensities are smaller than those required to observe Floquet-Bloch states, as here we need sufficient coupling with a continuum of states. From our numerics, for typical mid-infrared wavelengths (~ 160 meV) we estimate that intensities in the range of $1 - 10$ mW/ μm^2 would suffice.

Let us now discuss the influence of Rashba spin-orbit coupling. A Rashba term introduces spin-flip processes and it is a legitimate source of concern. Our numerical results evidence robustness of the photocurrents against this term (see supplementary information). This is because the mechanism relies on the existence of topologically protected states in the non-irradiated material, which are originated by intrinsic SOC and which extend to a region of parameters with moderate values of Rashba SOC. Indeed, the topological states are robust against a moderately strong Rashba SOC [1]: for $\gamma_R < 2\sqrt{e}\gamma_{SO}$ (γ_R and γ_{SO} being the strengths of the Rashba and intrinsic spin-orbit coupling terms) the resulting phase diagram is adiabatically connected to the quantum spin-hall phase of the Kane-Mele model. This topological protection is expressed in the fact that the matrix element between two topological counter-propagating states at one edge of any perturbation that preserves TRS is zero. In our case, circular polarization does not preserve TRS but rather than introducing a matrix element between counter-propagating edge states, leads to a selective hybridization of the edge states with the continuum at an energy differing by the photon energy from them. This is why our results are robust against spin non-conserving terms over a broad range of parameters.

Final remarks.— Using Floquet scattering theory we show how laser illumination can selectively disrupt the edge states of a two-dimensional topological insulator depending on their spin. This selectivity, which stems from the interplay between a spin-selective selection rule together with the hybridization of the edge states with the continuum of another Floquet replica, manifests by the generation of pure spin currents and spin-polarized charge photocurrents under linearly and circularly polarized laser-illumination, respectively. We emphasize that, in both cases, the spin and charge currents flow even at zero-bias voltage. Furthermore, the direction and spin polarization of these currents can be tuned by changing the incident electronic energy and the handedness of light polarization, thereby providing an experimental handle to control photocurrents. In this sense, given the generality of our model, we expect for the photocurrents predicted here to be experimentally accessible in two-dimensional materials by using laser illumination in the mid-infrared.

E.A.R.-M. acknowledges support by the ANID (Chile)PFCHA, DOCTORADO NACIONAL/2017, under ContractNo. 21171229. We thank the support of Fondecyt (Chile) under grant number 1170917, and by the EU Horizon 2020 research and innovation program under the Marie-Sklodowska-Curie Grant Agreement No. 873028 (HYDROTRONICS Project). L. E. F. F. T. also acknowledges the support of The Abdus Salam International Centre for Theoretical Physics and the Simons Foundation.

* These two authors contributed equally.

- [1] C. L. Kane and E. J. Mele, “Quantum Spin Hall Effect in Graphene,” *Phys. Rev. Lett.* **95**, 226801 (2005).
- [2] C. L. Kane and E. J. Mele, “ \mathbb{Z}_2 Topological Order and the Quantum Spin Hall Effect,” *Physical Review Letters* **95**, 146802 (2005).
- [3] B. A. Bernevig, T. L. Hughes, and S.-C. Zhang, “Quantum Spin Hall Effect and Topological Phase Transition in HgTe Quantum Wells,” *Science* **314**, 1757 (2006).
- [4] L. Fu and C. L. Kane, “Topological insulators with inversion symmetry,” *Phys. Rev. B* **76**, 045302 (2007).
- [5] M. König, S. Wiedmann, C. Brüne, A. Roth, H. Buhmann, L. W. Molenkamp, X.-L. Qi, and S.-C. Zhang, “Quantum Spin Hall Insulator State in HgTe Quantum Wells,” *Science* **318**, 766 (2007).
- [6] D. Hsieh, D. Qian, L. Wray, Y. Xia, Y. S. Hor, R. J. Cava, and M. Z. Hasan, “A topological Dirac insulator in a quantum spin Hall phase,” *Nature* **452**, 970 (2008).
- [7] Y. Ren, Z. Qiao, and Q. Niu, “Topological phases in two-dimensional materials: a review,” *Reports on Progress in Physics* **79**, 066501 (2016).
- [8] D. Kong and Y. Cui, “Opportunities in chemistry and materials science for topological insulators and their nanostructures,” *Nature Chemistry* **3**, 845 (2011).
- [9] F. Ortman, S. Roche, S. O. Valenzuela, and L. W. Molenkamp, eds., *Topological Insulators: Fundamentals and Perspectives* (Wiley, 2015).
- [10] X. Qian, J. Liu, L. Fu, and J. Li, “Quantum spin Hall effect in two-dimensional transition metal dichalcogenides,” *Science* **346**, 1344 (2014).
- [11] J. Liu, T. H. Hsieh, P. Wei, W. Duan, J. Moodera, and L. Fu, “Spin-filtered edge states with an electrically tunable gap in a two-dimensional topological crystalline insulator,” *Nature Materials* **13**, 178 (2014).
- [12] H. Pan, M. Wu, Y. Liu, and S. A. Yang, “Electric control of topological phase transitions in Dirac semimetal thin films,” *Scientific Reports* **5**, 14639 (2015).
- [13] W. G. Vandenberghe and M. V. Fischetti, “Imperfect two-dimensional topological insulator field-effect transistors,” *Nature Communications* **8**, 14184 (2017).
- [14] J. L. Collins, A. Tadich, W. Wu, L. C. Gomes, J. N. B. Rodrigues, C. Liu, J. Hellerstedt, H. Ryu, S. Tang, S.-K. Mo, S. Adam, S. A. Yang, M. S. Fuhrer, and M. T. Edmonds, “Electric-field-tuned topological phase transition in ultrathin Na₃Bi,” *Nature* **564**, 390 (2018).
- [15] D. Xiao, W. Yao, and Q. Niu, “Valley-Contrasting Physics in Graphene: Magnetic Moment and Topological Transport,” *Physical Review Letters* **99**, 236809 (2007).
- [16] T. Cao, G. Wang, W. Han, H. Ye, C. Zhu, J. Shi, Q. Niu, P. Tan, E. Wang, B. Liu, and J. Feng, “Valley-selective circular dichroism of monolayer molybdenum disulphide,” *Nature Communications* **3**, 887 (2012).
- [17] E. J. Sie, J. W. McIver, Y.-H. Lee, L. Fu, J. Kong, and N. Gedik, “Valley-selective optical Stark effect in monolayer WS₂,” *Nature Materials* **14**, 290 (2015).
- [18] H. Zeng, J. Dai, W. Yao, D. Xiao, and X. Cui, “Valley polarization in MoS₂ monolayers by optical pumping,” *Nature Nanotechnology* **7**, 490 (2012).
- [19] L. Zhang, K. Gong, J. Chen, L. Liu, Y. Zhu, D. Xiao, and H. Guo, “Generation and transport of valley-polarized current in transition-metal dichalcogenides,” *Physical Review B* **90**,

- 195428 (2014).
- [20] “Quantum phases on demand,” *Nature Physics* **16**, 1 (2020).
- [21] Y. H. Wang, H. Steinberg, P. Jarillo-Herrero, and N. Gedik, “Observation of Floquet-Bloch States on the Surface of a Topological Insulator,” *Science* **342**, 453 (2013).
- [22] F. Mahmood, C.-K. Chan, Z. Alpichshev, D. Gardner, Y. Lee, P. A. Lee, and N. Gedik, “Selective scattering between Floquet-Bloch and Volkov states in a topological insulator,” *Nature Physics* **12**, 306 (2016).
- [23] T. Oka and H. Aoki, “Photovoltaic Hall effect in graphene,” *Phys. Rev. B* **79**, 081406 (2009).
- [24] N. H. Lindner, G. Refael, and V. Galitski, “Floquet topological insulator in semiconductor quantum wells,” *Nat Phys* **7**, 490 (2011).
- [25] M. S. Rudner and N. H. Lindner, “Band structure engineering and non-equilibrium dynamics in Floquet topological insulators,” *Nature Reviews Physics* **2**, 229 (2020).
- [26] F. Giustino, M. Bibes, J. H. Lee, F. Trier, R. Valentí, S. M. Winter, Y.-W. Son, L. Taillefer, C. Heil, A. I. Figueroa, B. Plaças, Q. Wu, O. V. Yazyev, E. P. A. M. Bakkers, J. Nygård, P. Forn-Díaz, S. de Franceschi, L. E. F. Foa Torres, J. McIver, A. Kumar, T. Low, R. Galceran, S. O. Valenzuela, M. V. Costache, A. Manchon, E.-A. Kim, G. R. Schleder, A. Fazzio, and S. Roche, “The 2020 Quantum Materials Roadmap,” *Journal of Physics: Materials* (2020), 10.1088/2515-7639/abb74e.
- [27] J. W. McIver, B. Schulte, F.-U. Stein, T. Matsuyama, G. Jotzu, G. Meier, and A. Cavalleri, “Light-induced anomalous Hall effect in graphene,” *Nature Physics* **16**, 38 (2020).
- [28] M. Ezawa, “Photoinduced Topological Phase Transition and a Single Dirac-Cone State in Silicene,” *Physical Review Letters* **110**, 026603 (2013).
- [29] A. López, A. Scholz, B. Santos, and J. Schliemann, “Photoinduced pseudospin effects in silicene beyond the off-resonant condition,” *Phys. Rev. B* **91**, 125105 (2015).
- [30] M. Ezawa, “Monolayer Topological Insulators: Silicene, Germanene, and Stanene,” *Journal of the Physical Society of Japan* **84**, 121003 (2015).
- [31] H. L. Calvo, H. M. Pastawski, S. Roche, and L. E. F. Foa Torres, “Tuning laser-induced band gaps in graphene,” *Appl. Phys. Lett.* **98**, 232103 (2011).
- [32] H. L. Calvo, P. M. Perez-Piskunow, H. M. Pastawski, S. Roche, and L. E. F. Foa Torres, “Non-perturbative effects of laser illumination on the electrical properties of graphene nanoribbons,” *Journal of Physics: Condensed Matter* **25**, 144202 (2013).
- [33] A. Huamán and G. Usaj, “Floquet spectrum and two-terminal conductance of a transition-metal dichalcogenide ribbon under a circularly polarized laser field,” *Physical Review B* **99**, 075423 (2019).
- [34] M. Tahir, Q. Y. Zhang, and U. Schwingenshlögl, “Floquet edge states in germanene nanoribbons,” *Scientific Reports* **6**, 31821 (2016).
- [35] U. Bajpai, M. J. H. Ku, and B. K. Nikolic, “How robust is quantized transport through edge states of finite length: Imaging current density in Floquet topological vs. quantum spin and anomalous Hall insulators,” (2020).
- [36] A. Farrell and T. Pereg-Barnea, “Photon-Inhibited Topological Transport in Quantum Well Heterostructures,” *Physical Review Letters* **115**, 106403 (2015).
- [37] S. A. Sato, P. Tang, M. A. Sentef, U. De Giovannini, H. Hübener, and A. Rubio, “Light-induced anomalous Hall effect in massless Dirac fermion systems and topological insulators with dissipation,” *arXiv:1905.12981 [cond-mat, physics:physics]* (2019), arXiv: 1905.12981.
- [38] H. Sambe, “Steady States and Quasienergies of a Quantum-Mechanical System in an Oscillating Field,” *Phys. Rev. A* **7**, 2203 (1973).
- [39] G. Stefanucci, S. Kurth, A. Rubio, and E. K. U. Gross, “Time-dependent approach to electron pumping in open quantum systems,” *Phys. Rev. B* **77**, 075339 (2008).
- [40] L. Arrachea and M. Moskalets, “Relation between scattering-matrix and Keldysh formalisms for quantum transport driven by time-periodic fields,” *Phys. Rev. B* **74**, 245322 (2006).
- [41] L. E. F. Foa Torres, P. M. Perez-Piskunow, C. A. Balseiro, and G. Usaj, “Multiterminal Conductance of a Floquet Topological Insulator,” *Phys. Rev. Lett.* **113**, 266801 (2014).
- [42] M. Moskalets and M. Büttiker, “Floquet scattering theory of quantum pumps,” *Phys. Rev. B* **66**, 205320 (2002).
- [43] B. L. Altshuler and L. I. Glazman, “Pumping Electrons,” *Science* **283**, 1864 (1999).
- [44] F. Giazotto, P. Spathis, S. Roddaro, S. Biswas, F. Taddei, M. Governale, and L. Sorba, “A Josephson quantum electron pump,” *Nature Physics* **7**, 857 (2011).
- [45] B. Kaestner and V. Kashcheyevs, “Non-adiabatic quantized charge pumping with tunable-barrier quantum dots: a review of current progress,” *Reports on Progress in Physics* **78**, 103901 (2015).
- [46] U. Bajpai, B. S. Popescu, P. Plecháč, B. K. Nikolić, L. E. F. F. Torres, H. Ishizuka, and N. Nagaosa, “Spatio-temporal dynamics of shift current quantum pumping by femtosecond light pulse,” *Journal of Physics: Materials* **2**, 025004 (2019).
- [47] L. E. F. Foa Torres, V. Dal Lago, and E. Suárez Morell, “Crafting zero-bias one-way transport of charge and spin,” *Physical Review B* **93**, 075438 (2016).
- [48] V. Dal Lago, E. Suárez Morell, and L. E. F. Foa Torres, “One-way transport in laser-illuminated bilayer graphene: A Floquet isolator,” *Physical Review B* **96**, 235409 (2017).
- [49] M. Berdakin, J. E. B. Vargas, and L. E. F. Foa Torres, “Directional control of charge and valley currents in a graphene-based device,” *Physical Chemistry Chemical Physics* **20**, 28720 (2018).
- [50] O. Balabanov and H. Johannesson, “Transport signatures of symmetry protection in 1D Floquet topological insulators,” *J. Condens. Matter Phys.* **32**, 015503 (2019),.
- [51] K. Ghalamkari, Y. Tatsumi, and R. Saito, “Perfect Circular Dichroism in the Haldane Model,” *Journal of the Physical Society of Japan* **87**, 063708 (2018).
- [52] F. D. M. Haldane, “Model for a Quantum Hall Effect without Landau Levels: Condensed-Matter Realization of the “Parity Anomaly,”” *Phys. Rev. Lett.* **61**, 2015 (1988).